Cell Reports
Physical Science

CellPress
OPEN ACCESS

Article

Thermodynamic loss analysis of a liquid-sorbent direct air carbon capture plant

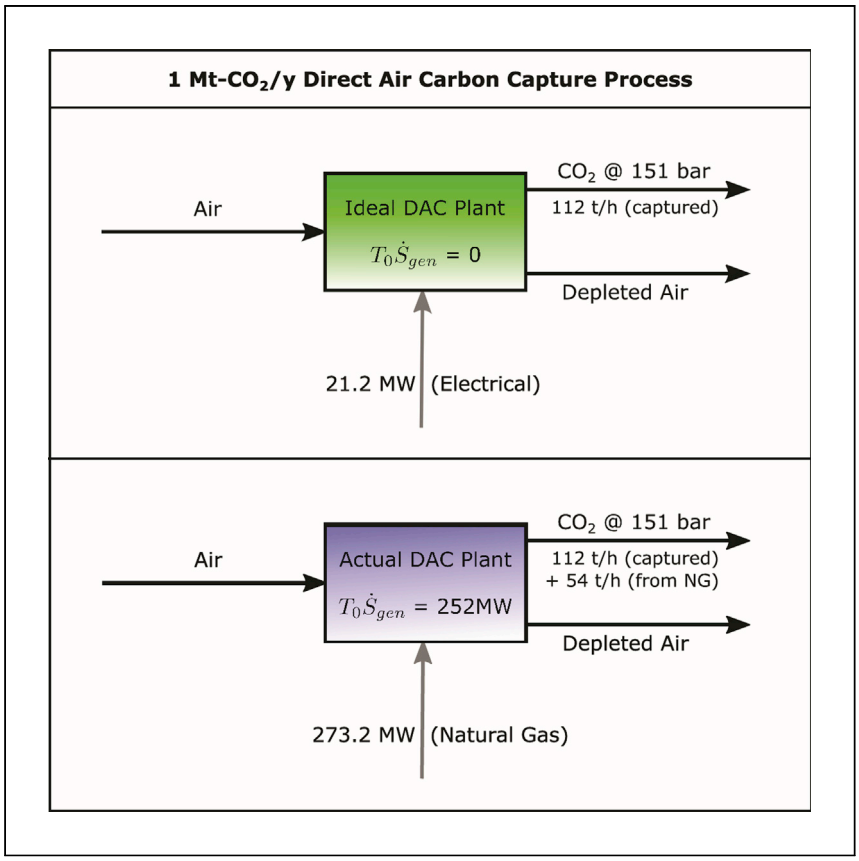

Direct air carbon capture plants' high energy consumption may be argued as prohibitive to their large-scale deployment. Here, Long-Innes and Struchtrup analyze the thermodynamic losses/exergy destruction at a system and component level for a natural-gas-fueled plant and discuss the loss mechanisms' implications for process improvements and energy usage reductions.

Ryan Long-Innes, Henning Struchtrup

struchtr@uvic.ca

Highlights

Full thermodynamic evaluation of a natural-gas-fueled liquid-sorbent DAC plant

Total destroyed exergy of 252 MW for 273.2 MW provided, second-law efficiency of 7.8%

Largest irreversible losses due to dissipation of chemical exergy as low-grade heat

Evaluation and discussion of thermodynamic losses for all individual components

Long-Innes & Struchtrup, Cell Reports Physical Science 3, 100791
March 16, 2022
https://doi.org/10.1016/j.xcrp.2022.100791

Cell Reports
Physical Science

CellPress
OPEN ACCESS

Article

Thermodynamic loss analysis of a liquid-sorbent direct air carbon capture plant

Ryan Long-Innes[1] and Henning Struchtrup[1,2,*]

SUMMARY

Direct air capture of CO_2 is often presented as a promising technology to help mitigate climate change, although proposed processes are highly energy intensive. We analyze Carbon Engineering's 1 Mt-CO_2/year natural-gas-powered direct air capture (DAC) process, which requires 273.2 MW per plant, where we find that 252 MW are irreversibly lost, corresponding to a second-law efficiency of 7.8%. Our component-level analysis details the mechanisms by which these losses of thermodynamic work potential occur in the most energy-intensive plant segments. Here, we emphasize the effects of chemical exergy dissipation in the air contactor, where stored chemical exergy is released as low-grade heat into the environment. Other major losses occur in the calciner and its preheat cyclones due to the high temperature demanded by its internal chemical reaction, as well as in the water knockout system, CO_2 compression system, and power island. Finally, we illustrate the issues arising from the use of natural gas as a feedstock for heat and power, and suggest directions to pursue for further analysis and process improvements, which we consider imperative to make this DAC process a viable option for large-scale CO_2 removal toward IPCC targets.

INTRODUCTION

According to studies from the Intergovernmental Panel on Climate Change (IPCC), carbon dioxide removal (CDR) technologies play significant roles[1] in all pathways examined to limit a global temperature rise of 1.5°C. As global CO_2 emissions continue to rise, interest in technologies designed to actively remove the gas from the atmosphere is becoming increasingly prevalent. One of the most promising of these negative-emissions technologies under development, known as direct air capture (hereafter referred to as DAC), uses solid-sorbent or aqueous-sorbent filters to sequester carbon dioxide directly from atmospheric air. The CO_2 may subsequently be pumped underground for permanent geological storage or used for various industrial and chemical processes, production of synthetic hydrocarbon fuels, or enhanced oil recovery.[2]

DAC, while appearing to be a promising technology, faces many challenges. With the amount of CO_2 in atmospheric air being very dilute, DAC requires massive amounts of energy per unit of CO_2 captured, incurring significant energy costs in processing large volumes of air and in regeneration of the sorbent material. Partly as a result of this high energy demand, it becomes a rather cost-intensive process.

The Canadian company Carbon Engineering has proposed an aqueous-sorbent-based chemical looping process for DAC,[3] capable of capturing 0.98 Mt-CO_2/year

[1]Department of Mechanical Engineering, University of Victoria, Victoria, BC V8P 5C2, Canada

[2]Lead contact

*Correspondence: struchtr@uvic.ca

https://doi.org/10.1016/j.xcrp.2022.100791

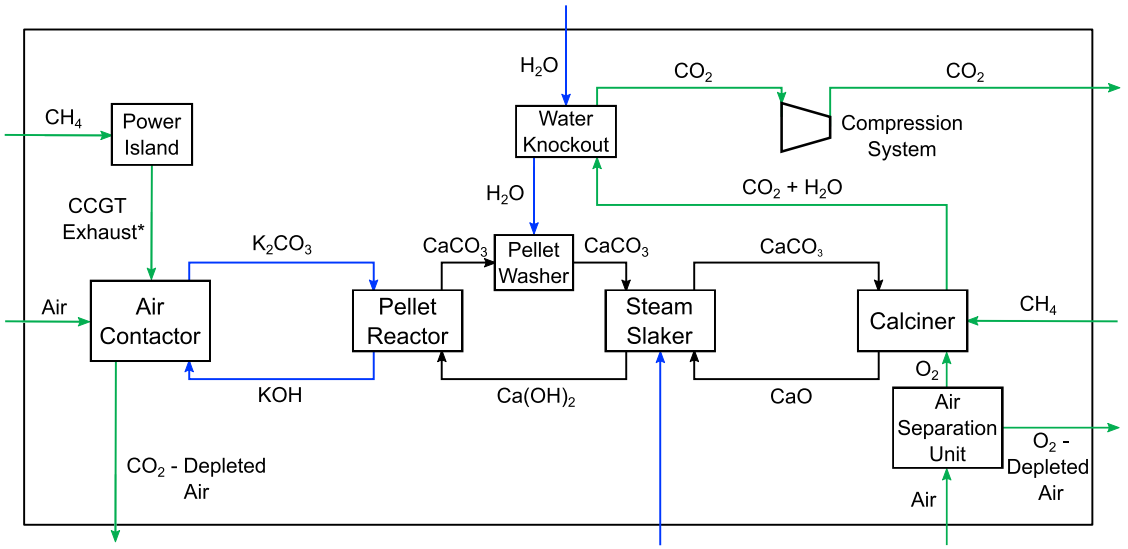

Figure 1. Simplified process schematic of Carbon Engineering's 1 Mt-CO_2/year DAC plant

Main material and chemical flows are indicated; see Keith et al.[3] for the complete process diagram. Exhaust gas from the CCGT system passes through a separate CO_2 absorber (coupled to the pellet reactor's KOH loop) to partially capture its CO_2 content prior to its passage through the air contactor;[3] we omit it here for illustrative purposes.

(111.9 t-CO_2/h). For our analysis, their plant design is selected because of its scalability and its publicly available process data. A simplified schematic of their natural-gas-powered ("A" configuration)[3] plant design is shown in Figure 1. A more detailed plant schematic, as used for the process analysis in this paper, is presented in Keith et al.[3]

The process begins with atmospheric air being drawn by large fans into the air contactor, in which it is exposed to sorbent material wetted with potassium hydroxide (KOH) in solution. The air's CO_2 content reacts with the potassium hydroxide to yield potassium carbonate (K_2CO_3) and water, forming an aqueous solution.

This solution is then passed to a pellet reactor, in which it is precipitated with calcium hydroxide ($Ca(OH)_2$) to form solid pellets of calcium carbonate ($CaCO_3$) along with potassium hydroxide (KOH) for reuse. The calcium carbonate pellets are washed to remove residual KOH, partially preheated by the steam slaker, and finally transported to the calciner: here, CO_2 is released from calcium carbonate through calcination, i.e., heat input at high temperature, through oxy-fuel combustion of natural gas (primarily CH_4) with 95.60% pure oxygen gas, the oxygen being provided by a cryogenic air separation unit (ASU). Lime, or calcium oxide (CaO), being the other product of calcination, is slaked with water in the steam slaker to produce calcium hydroxide for the pellet reactor, hence completing Carbon Engineering's chemical loop system.

A portion of the water vapor in the calciner's outgoing gas stream, produced as a combustion product, is removed via the water knockout drum, the remainder being removed in the four-stage compression system's intercooling stages. The concentrated CO_2 stream then leaves the compression system (and the plant) at[3] 151 bar.

In Figure 1, the power island encompasses a combined-cycle gas turbine (CCGT) system and steam turbine integrated into the plant's major components, i.e., the

CO_2 from the gas turbine exhaust is also absorbed in the KOH solution, while the steam turbine is fed with steam from slaker and heat recovery steam generator (HRSG), superheated through heat exchange with the calciner's outgoing gas stream.

Carbon Engineering estimates the net levelized cost to range between (2016 USD) \$94 and \$232 per t-CO_2 captured from the atmosphere, the lower value assuming a 7.5% capital recovery factor (CRF) with natural gas and grid electricity used to produce CO_2 at 0.1 MPa, the upper assuming a 12.5% CRF with an electrically neutral plant (only natural gas used for energy) producing pipeline-ready[3] CO_2 at 15 MPa.

According to the 2019 committee report published by the National Academies of Sciences, Engineering, and Medicine, to meet Paris Agreement targets for atmospheric greenhouse gas reduction[4] without significant detriment to global economic growth, carbon removal technologies such as DAC will need to remove[5] 10 Gt-CO_2/year from the atmosphere by 2050 and 20 Gt-CO_2/year by 2100. By simple calculation using Carbon Engineering's levelized cost range, removal of these amounts using their technology would correspond to a net cost range of \$940 billion to \$2.32 trillion/year by 2050, or \$1.88 trillion to \$4.62 trillion/year by 2100 (in 2016 USD). For comparative purposes, using CPI inflation-adjusted[6] costs of \$85–\$211/t-CO_2 in 2010 USD as a baseline (due to available GDP data),[7] this amounts to 1.0%–2.5% of 2019's global real GDP of \$84.97 trillion (2010 USD)[7] by 2050, or 2.0%–5.0% by 2100.

Carbon Engineering's calculations[3] assume a fixed natural gas cost of \$3.50/GJ for their baseline A (natural gas) configuration; with gas input at 8.81 GJ/t-CO_2, energy input accounts for \$30.84/t-CO_2. For their lowest-cost configuration, gas input at 5.25 GJ/t-CO_2 accounts for \$18.38/t-CO_2 and grid electricity, priced between \$30 and \$60/MWh, accounts for \$2.31–\$4.62/t-CO_2. At the 2050 removal rate target, with their existing technology, their A configuration would require a natural gas input of 8.81×10^{10} GJ/year (2.36 trillion Nm^3/year), or 58% of 2019's global natural gas production[8] of 4.089 trillion Nm^3. Such massive demand would certainly increase the price of the commodity and would present tremendous logistical challenges to widespread deployment.

With energy costs contributing a significant portion of the net cost of capture, and because energy consumption in the existing design could be argued to be prohibitive to large-scale deployment, in this report we identify the segments of the plant in which the largest work losses due to irreversibilities occur, i.e., the primary system components that energy efficiency improvement measures must target.

Our analysis will show that, with respect to energy input, the process is affected by large irreversible losses totaling 252 MW across the system, corresponding to a second-law efficiency of 7.8% given an environmental temperature of 21°C. Analysis of the individual components then follows, where we discuss the mechanisms by which these losses occur and quantify individual contributions to the net work loss. We find the largest losses to be due to dissipation of chemical exergy, external to the calciner, as low-grade heat (~39.4% of total losses); the calciner itself (25%); and the CCGT power island (16.4%). All losses quantified are presented in Table 1.

Finally, we summarize our results and discuss their implications for large-scale implementation of DAC technology, including brief estimates of energy consumption when substituting natural gas with renewable energy sources.

Table 1. Major losses to irreversibilities in Carbon Engineering's 1 Mt-CO_2/year plant as percentages of total thermodynamic loss and of total loss less water evaporation

Source of loss	Irrev. loss $\dot{W}_{loss}$ (MW)	% of $\dot{W}_{loss}^{tot}$	% of $\dot{W}_{loss}^{NG}$
Chemical exergy dissipation (ext. to calciner) + other	99.3	38.5%	39.4%
Calciner	63.0	24.4%	25.0%
Combined-cycle gas turbine	41.5	16.1%	16.4%
Steam turbine	11.0	4.3%	4.4%
Air separation unit	10.4	4.0%	4.1%
Compression system	9.8	3.8%	3.9%
Air contactor fans	9.2	3.6%	3.7%
Water knockout	7.8	3.0%	3.1%
Air contactor evaporation	6	2.3%	–
Total	258	100%	100%

RESULTS AND DISCUSSION

Theoretical framework

Thermodynamic analysis of Carbon Engineering's 1 Mt/year plant was performed by applying mass, energy, and entropy balances over each relevant component or subsystem, with Carbon Engineering's published simulation results[3] providing known quantities where necessary.

For all cases presented, balance equations assume steady-state operation of the plant, i.e., all time derivatives vanish. Energy balances neglect changes in kinetic and potential energy, considering only enthalpic differences between incoming and outgoing chemical species flows to have an effect on rates of work and heat exchange.

The mass, energy, and entropy balances thus assume the following respective forms:[9]

$$\sum_{out} \dot{m}_e = \sum_{in} \dot{m}_i, \qquad \text{(Equation 1)}$$

$$\sum_{out} \dot{n}_e \overline{h}_e - \sum_{in} \dot{n}_i \overline{h}_i = \dot{Q}_0 + \sum_k \dot{Q}_k - \dot{W}, \qquad \text{(Equation 2)}$$

$$\sum_{out} \dot{n}_e \overline{s}_e - \sum_{in} \dot{n}_i \overline{s}_i - \frac{\dot{Q}_0}{T_0} - \sum_k \frac{\dot{Q}_k}{T_k} = \dot{S}_{gen} \geq 0, \qquad \text{(Equation 3)}$$

where $\dot{m}$ denotes mass flow rate, $\dot{n}$ mole flow rate, $\overline{h}$ molar specific enthalpy, $\overline{s}$ molar specific entropy, $\dot{W}$ rate of work (power), $\dot{Q}_k$ heat transfer rate over a system boundary at temperature T_k, and $\dot{S}_{gen}$ the rate of entropy generation in the system. These equations are valid for all open systems and subsystems considered in our analysis.

For any variable x, we use the notation $\dot{x}$ to represent its transfer rate, e.g., a time-invariant quantity of work is denoted W, while rate of work (power) is denoted $\dot{W}$. Because we rarely speak in terms of time-invariant quantities throughout our analysis, terms such as "work potential," "reversible work," and "work loss" often refer to rates of work. To avoid confusion when discussed, time-invariant quantities of work and heat will always be preceded with qualifiers such as "mass-specific," "mole-specific," etc.

Note that in Equations (2) and (3), we isolate the term $\dot{Q}_0$, which is the heat exchange with the external environment at temperature T_0 (we choose 21°C),[3] the

environment being considered a freely available heat source/sink. From here, we eliminate $\dot{Q}_0$ between Equations (2) and (3) to find power as:

$$\dot{W} = -T_0\dot{S}_{gen} + \sum_k \left(1 - \frac{T_0}{T_k}\right)\dot{Q}_k + \sum_{in} \dot{n}_i(\bar{h}_i - T_0\bar{s}_i) - \sum_{out} \dot{n}_e(\bar{h}_e - T_0\bar{s}_e). \quad \text{(Equation 4)}$$

In Equation (4), work loss to irreversibilities is represented by:[9]

$$\dot{W}_{loss} = T_0\dot{S}_{gen} \geq 0, \quad \text{(Equation 5)}$$

where, according to our sign convention, $\dot{W}_{loss}$ increases power requirements for power-consuming systems and decreases power output for power-producing systems.

For fully reversible systems, for which entropy generation $\dot{S}_{gen}$ vanishes, Equation (4) gives the minimum possible power requirement ($\dot{W}$ <0) for power-consuming components/systems, or the highest possible power output ($\dot{W}$>0) for power producing systems, i.e., thermodynamically reversible work.

Overall, in irreversible thermodynamic processes, entropy is generated, reducing the efficiency of energy conversion. In the context of the systems we analyze, irreversibilities primarily occur owing to undesired heat transfer, uncontrolled chemical reactions, mixing of chemical streams, and friction.

Equation (4) can also be written as:

$$\dot{W} = \dot{W}_{rev} - \dot{W}_{loss}, \quad \text{(Equation 6)}$$

where, for the present energy-consuming application, actual work ($\dot{W}$) and reversible work ($\dot{W}_{rev}$) are inputs and are therefore negative, while the loss ($\dot{W}_{loss}$) is a positive quantity such that it increases the actual work required. Depending on the nature and magnitude of irreversibilities, the actual work requirement can be substantially larger than the minimum required, i.e., reversible, work. This is indeed the case for DAC at a system level.

A useful measure for process quality is the second-law efficiency, which measures the ratio between minimum work requirement and actual work requirement in practice:[9]

$$\eta_{II} = \frac{|\dot{W}_{rev}|}{|\dot{W}|} = \frac{|\dot{W}_{rev}|}{|\dot{W}_{rev}| + |\dot{W}_{loss}|}. \quad \text{(Equation 7)}$$

While a high second-law efficiency does not always imply optimality of a process with respect to financial constraints, the DAC process that minimizes energy consumption, which indeed this publication focuses on, will also minimize irreversible losses, i.e., maximize second-law efficiency, as much as is economically feasible.

Reversible work for separation

To begin, it is necessary to review the concept of thermodynamic reversible work requirements in the context of DAC, particularly to illustrate the power-requirement implications of carbon dioxide's dilute atmospheric concentration.

Carbon Engineering's 1 Mt-CO_2/year plant is designed to remove 111.9 t-CO_2/h from the atmosphere,[3] from a mass flow of 251,000 t-air/h with 0.060 mass-% CO_2. Given these data, their simulation was performed to correspond with an atmospheric CO_2 mole fraction of $X^i_{CO_2} = 0.000391 = 391$ ppm. While recent measurements[10] give 416 ppm as of August 2021, we will use 391 ppm to maintain conservative work estimates and to stay consistent with Carbon Engineering's data.

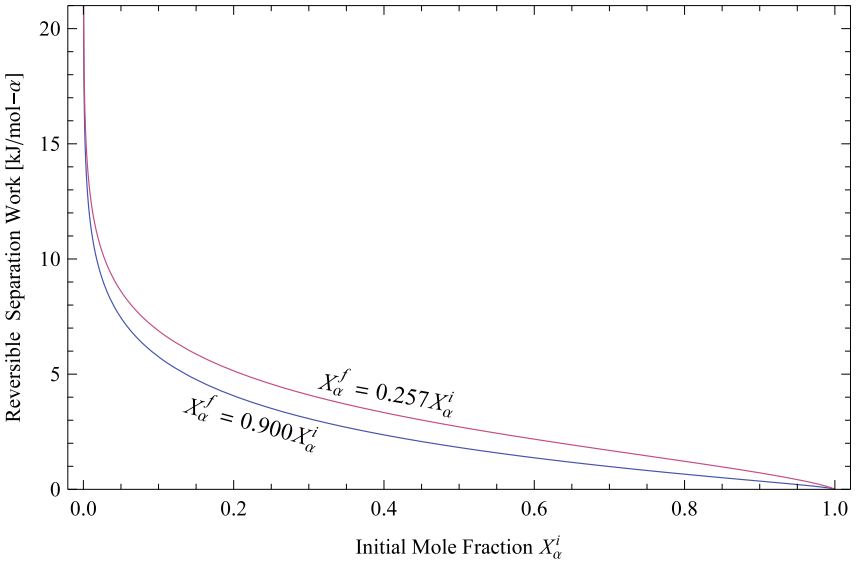

Figure 2. Reversible mole-specific separation work versus initial gas mole fraction at T_0 = 294 K

Two curves are plotted, one representing a final mole fraction of $X_\alpha^f = 0.90 X_\alpha^i$ in the gas stream (removal of 10% of the gas). The other was set to $X_\alpha^f = 0.257 X_\alpha^i$ (removal of 74.3% of the gas) to correspond with the Carbon Engineering plant's capture fraction.

Figure 2 shows the relationship between the initial mole fraction X_α^i of a component α, i.e., CO_2, in an ideal gas stream and the minimum mole-specific work required for its isolation, considering no changes to total pressure and temperature.

As can be seen in Figure 2, as the initial mole fraction of a component in a gas stream decreases, the minimum amount of mole-specific work required to separate it from the other components of the gas increases exponentially. With temperature and pressure remaining constant, separation work is driven entirely by entropy of mixing.

For comparative purposes, with component α being CO_2 at 21°C, separation from flue gas in a coal-fired power plant with $X_{CO_2}^i$ = 0.15 requires[11] a minimum of 5.87 kJ/mol-CO_2 (133 MJ/t-CO_2) to reduce its mole fraction by 74.3%. Separation from atmospheric air with $X_{CO_2}^i$ = 0.000391, as in Carbon Engineering's case, requires a minimum of 20.48 kJ/mol-CO_2 (465 MJ/t-CO_2) to reduce its mole fraction by 74.3%, an $\sim$ 3.5× increase.

At first glance, the factor of 3.5 may not appear to be a significant difference. However, considering that the initial mole fractions in this comparison differ by three orders of magnitude, for every mole of CO_2 the DAC sorbent material is exposed to, 2,557 mol of air must pass through the contactor. In contrast, only 6.67 mol of flue gas must pass through the power plant's sorbents to expose them to 1 mol of CO_2. Thus, while reversible separation work does not appear to be penalized significantly on a molar basis, the actual rates of work for DAC are implied to be much larger due to a 380× increase in the incoming gas stream's required molar flow rate—significant amounts of power (9.2 MW in Carbon Engineering's process)[3] must be dedicated simply to moving massive volumes of air through the sorbent material.

It should also be noted that, while the use of a weak base in the air contactor solution should theoretically result in lower energy demand for sorbent regeneration,[12] a

substantial increase in contactor area would be required as a consequence,[13] and with it a proportional increase in fan power. The use of a strong base, as in Carbon Engineering's case, implies smaller contactor area compared with the weak-base approach, although a much higher quality of thermal energy for regeneration is required.[13]

Caram et al. introduced an approach to determine reversible work based on the energy required for this regeneration step.[12] Our approach instead is to compare Carbon Engineering's plant to a generalized reversible DAC process based solely on entropy of mixing, i.e., the plot in Figure 2.

For Carbon Engineering's plant to remove 111.9 t-CO_2/h from its incoming airstream, we find a thermodynamic minimum power requirement of 14.46 MW for pure CO_2 leaving the plant at 21°C and 1 bar. Because the CO_2 is pressurized to 151 bar for pipeline transport and sequestration,[3] we add the reversible work/power for isothermal compression (6.74 MW) to find the plant's total reversible work requirement:

$$\left|\dot{W}_{\text{rev}}^{\text{tot}}\right| = 21.20\ \text{MW}.$$

Reversible natural gas use for CO_2 separation

Still considering a reversible process, we ask for the amount of natural gas required for reversible CO_2 separation at 21°C. We estimate the natural gas mass flow rate by considering the mole-specific work potential of CH_4, which is, for combustion with pure O_2, simply its Gibbs free energy of reaction:

$$\triangle \overline{g}_R(294\text{K},\ 1\ \text{atm}) = -800.8\text{kJ/mol}.$$

Here, we discount the additional work that may be obtained through reversible mixing of the combustion product stream.[9] Taking the quotient of the reversible work requirement (21.20 MW) and the mole-specific work potential gives a 1.53 t/h flow of CH_4, or 13.7 kg-CH_4/t-CO_2 separated for a 111.9 t-CO_2/h capture rate.

In practice, that is, for the actual irreversible plant, a 19.7 t/h flow of CH_4 is required[3] (or 176.1 kg-CH_4/t-CO_2), corresponding to a work potential of 273.2 MW by the same calculation method.

Thus, for removal of 10 Gt-CO_2/year using a *fully reversible* process relying on only natural gas, an input of 13.7 Mt-CH_4/year (or $\sim 2.06 \times 10^{11}$ Nm^3/year) would be required. This would still be a substantial portion of yearly global production, corresponding to ~5.04% of 2019's production[8] of 4.089×10^{12} Nm^3.

With the actual process set to consume ~11.5 times more than this, one can expect that widespread deployment of DAC plants relying solely on natural gas as a feedstock would prove problematic from a resource-consumption perspective. In addition to this, the potential for fugitive methane emissions, both in upstream processing and within the plant, may hamper the plant design's negative-emissions credentials; indeed, the worst case would see a DAC plant that has more CO_2-equivalent methane emissions than the actual CO_2 it removes from the atmosphere.

Net work loss and second-law efficiency

To estimate net work loss and second-law efficiency, we apply Equation (4) over the entirety of the Carbon Engineering plant. Because all power is produced internally through the use of natural gas as feedstock (no external work input, $\dot{W} = 0$), we find the net work loss as the total difference in $\dot{n}(\overline{h} - T_0\overline{s})$ terms in Equation (4) for

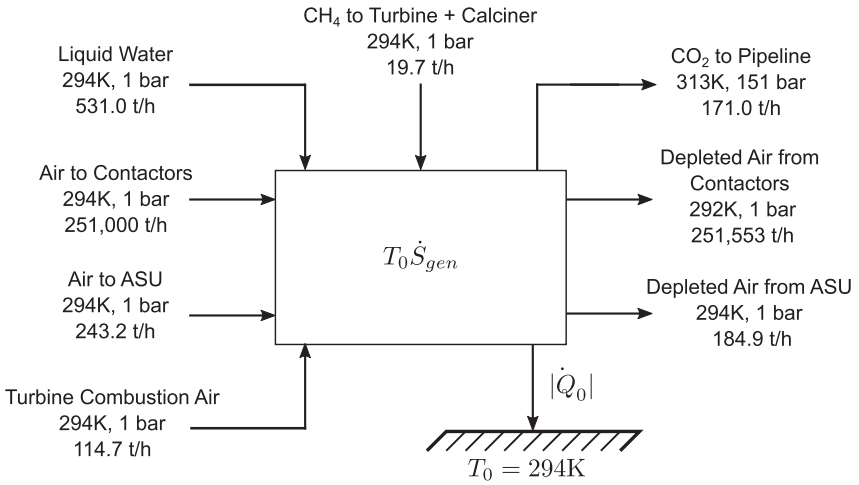

Figure 3. System-level flow diagram of Carbon Engineering's baseline DAC plant configuration

The outgoing "CO_2 to pipeline" stream comprises[3] 97.12% CO_2, 1.36% O_2, 1.51% N_2, and 0.01% H_2O. "Air to ASU" and "depleted air from ASU" streams were computed by mass and energy balances over the ASU (see Note S2), while the "turbine combustion air" stream assumed stoichiometric combustion to produce Carbon Engineering's reported CCGT outflows.[3]

all flows entering and leaving the system. Figure 3 shows all inflows to and outflows from Carbon Engineering's plant.

The natural gas configuration requires an ASU for fluidized-bed combustion with pure O_2 in the calciner, ensuring that combustion products consist primarily of CO_2 and water. We assume the ASU's air supply contains a quantity of oxygen equal to that which is fed to the calciner (55.93 t/h), giving an incoming flow rate of 243.2 t/h for air containing 23% O_2 by mass.

In addition, while the Carbon Engineering plant diagram gives a 252,000 t/h mass flow leaving the air contactor,[3] we use the non-rounded value of 251,553 t/h as obtained by mass balance with all other inflows/outflows of Figure 3.

For the system as shown in Figure 3, from Equations (4) and (5) we find the net work loss to entropy generation:

$$\dot{W}^{\text{tot}}_{\text{loss}} = 258\ \text{MW}.$$

Together with the 21.20 MW reversible work requirement, this yields

$$\dot{W}^{\text{tot}}_{\text{loss}} + \left|\dot{W}^{\text{tot}}_{\text{rev}}\right| = 279.2\ \text{MW}$$

as the overall work potential consumed by the system.

We point out that, while the system consumes 273.2 MW of work potential from natural gas, the air contactor sees liquid water evaporating into the passing air, which then leaves as vapor in the depleted airstream. This uncontrolled evaporation destroys ~4.2 MW of work potential for the case of adiabatic evaporation (in which case the air-liquid mixture would leave at 16°C) to ~7.9 MW for isothermal evaporation (the mixture leaving at 21°C). Taking the difference between the overall work potential consumed (279.2 MW) and the process fuel's work potential (273.2 MW), we estimate this additional loss to evaporation to be ~6 MW (or 2.3% of $\dot{W}^{\text{tot}}_{\text{loss}}$), which our calculation for $\dot{W}^{\text{tot}}_{\text{loss}}$ implicitly includes.

We do not consider this evaporative loss to be meaningful in the context of the process's evaluation, as the work being "paid for" is the energy supply, with the exergy lost to evaporation being unharvestable regardless. Thus, we also define the net loss quantity:

$$\dot{W}_{\text{loss}}^{NG} = 258\ \text{MW} - 6\ \text{MW} = 252\ \text{MW},$$

which is the work lost from the work potential provided by natural gas. In this way the second-law efficiency, whose denominator should equal the actual work requirement in practice (Equation [7]), is not penalized due to losses unassociated with the process's energy source.

Using $\dot{W}_{\text{loss}}^{NG} = 252$ MW in Equation (7) with the plant's reversible work requirement (21.20 MW) gives the second-law efficiency:

$$\eta_{II} = 0.078 = 7.8\%.$$

For the natural gas A configuration with CO_2 compression to 151 bar, this can be interpreted as the plant in practice consuming ~13× more energy than is theoretically required. This value agrees with other estimates for second-law efficiency of KOH-sorbent DAC processes, Sabatino et al.[14] giving 7.6%–7.9%.

Thus, opportunities are available to reduce power/heat consumption, and therefore cost per unit of CO_2 captured, through revision of the plant's internal processes; these will be explored and discussed in the component-level analysis section.

It should also be noted that heat exchange with the environment, that is, $|\dot{Q}_0|$, Figure 3, is strongly dependent on the temperature of the CO_2-depleted air leaving the air contactor, the temperature being below T_0 = 21°C due to evaporative cooling. For the given value of 19°C, $|\dot{Q}_0|$ = 75 MW, while for a 1°C increase to 20°C, $|\dot{Q}_0|$ = 0. Work loss to entropy generation is affected by these changes to a much smaller degree, however, with the 1°C increase adding only an additional 0.4 MW of work loss.

Calciner and preheat cyclones

We begin the component level analysis with the calciner, the most energy-demanding component, with a total energy input of 186.91 MW, 99.6% of which is in the form of combustion heat.[3] The calciner's high thermal demand is largely unavoidable due to the high reaction enthalpy required for decomposition of calcium carbonate to calcium oxide and carbon dioxide ($CaCO_{3(s)} \rightarrow CaO_{(s)} + CO_{2(g)}$, standard enthalpy of reaction $\triangle \overline{h}_R$ = 179kJ/mol).

Figure 4 shows the calciner and preheater system as adapted from Carbon Engineering's data. All flows enter and leave the system at atmospheric pressure, with the exception of the oxygen stream from the ASU, which is provided at 120 kPa. Due to lack of data available for the preheat cyclones (PH1, PH2, and PH3), they are treated as adiabatic with perfect heat exchange between flows, i.e., all flows exiting at the same temperature. For consistency with Carbon Engineering's simulation data, we omit the small flow of filtered $CaCO_3$ fines from the pellet reactor as an incoming flow to the first preheater.[3] With these assumptions, the resulting temperatures found, as labeled in Figure 4, are reasonably close to those obtained by Carbon Engineering in their simulation, the largest discrepancy being 642°C as the highest possible temperature at which flows may leave the second preheater. For this value, Carbon Engineering reports[3] 650°C.

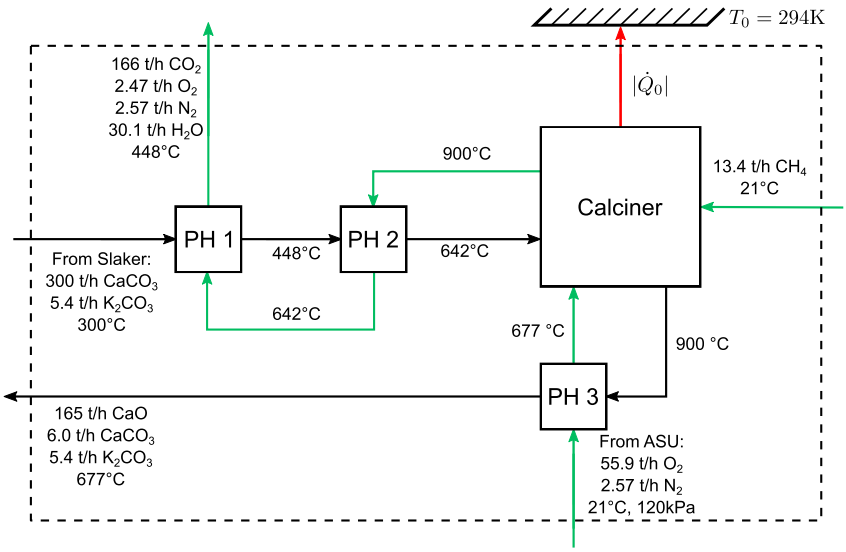

Figure 4. Calciner and preheat system for natural gas configuration

Gas flows are shown in green, solid flows are shown in black, Heat transfer to the environment is shown in red.

Applying the energy balance to the system shown, we find a net heat loss $|\dot{Q}_0| =$ 6.6 MW to the environment at 21°C. Through the entropy balance Equation (4), we find:

$$\dot{W}_{\text{loss}}^{\text{calc}} = 63 \text{ MW } (25.0\% \text{ of } \dot{W}_{\text{loss}}^{NG}),$$

that is, 63 MW of destroyed work potential due to irreversible chemical reaction, i.e., chemical exergy dissipation, and heat transfer between gaseous and solid material flows. Further discussion on calciner heat transfer as it relates to thermal demand and work loss is available in Long-Innes.[15]

To estimate the thermal efficiency of the calciner, we compared existing data to an idealized system in which reactant ($CaCO_3$) and product (CaO and CO_2) enter and leave at 300°, respectively, and react at 900°C. We found this simplified system to require 145 MW of heat, of which 136 MW is used to sustain the $CaCO_3$ decomposition reaction, the remainder being the net amount consumed in preheating and cooling the pellet stream. Using this 145 MW as a baseline to compare its actual 186.11 MW thermal demand, we found the calciner to be 78% thermally efficient, consistent with Carbon Engineering's value.[3]

We note that reduction of the calciner's internal pressure would indeed correspond to a reduction in required operating temperature by the law of mass action,[9] and therefore would reduce its thermal demand. However, due to the near-vacuum pressures required to accomplish a substantial decrease in equilibrium temperature for $CaCO_3$ decomposition, calciner pressure reduction may be argued to be an unproductive route to pursue for process improvement (see Note S1 for details).

Air separation unit

The ASU produces a flow of 58.5 t/h of gas mixture, primarily oxygen (95.60% by mass), and requires 13.3 MW of power,[3] corresponding to ~58% of the plant's reversible work requirement. Applying the conservation laws, where we assume waste gas from air purification (N_2, CO_2, and H_2O) leaves at the same temperature

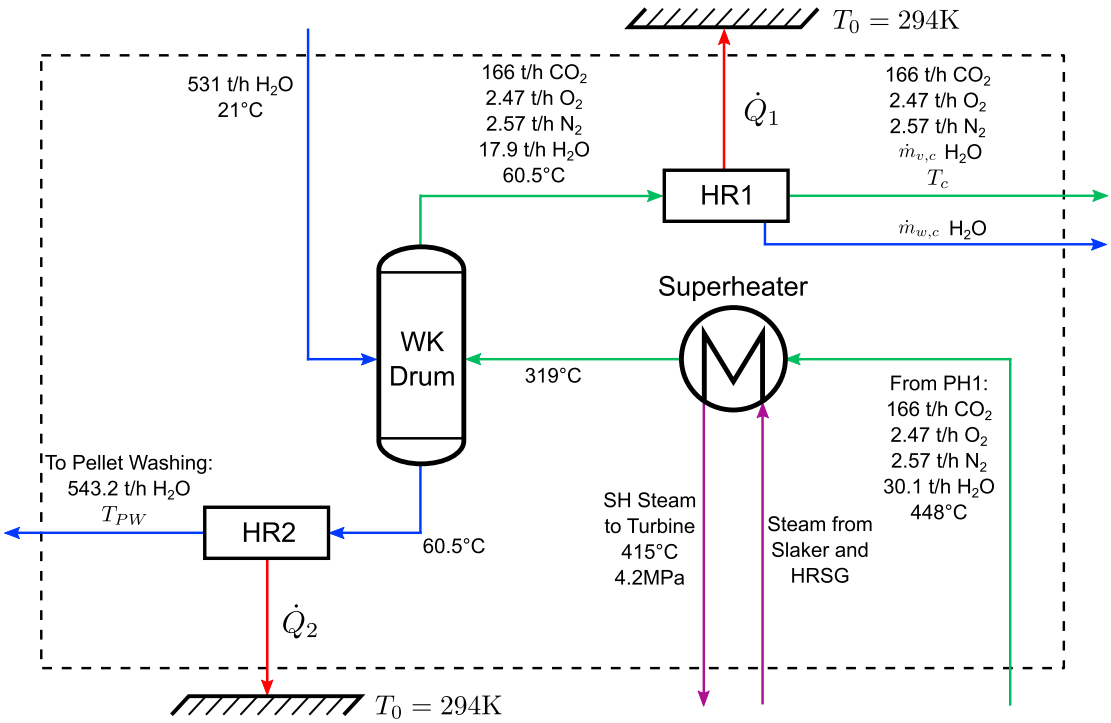

Figure 5. Superheater and water knockout drum for natural gas configuration
Gas flows shown in green, liquid water in blue, steam in purple, and heat in red.

and pressure at which it originally enters, we find the reversible work requirement for the ASU to be $|\dot{W}_{rev}| = 2.9$ MW. This value corresponds[3] to a pressurized product stream at 120 kPa, giving a second-law efficiency of 21.8% for the ASU. For an unpressurized product stream, we find only a small difference, where $|\dot{W}_{rev}| = 2.7$ MW. Due to the inherent difficulty of air separation, requiring large temperature and pressure swings for liquefaction and fractional distillation, the ASU contributes a substantial irreversible work loss of

$$\dot{W}_{loss}^{ASU} = 10.4 \text{ MW } (4.1\% \text{ of } \dot{W}_{loss}^{NG}).$$

Its detailed calculation is available in Note S2, where it is shown as an example of our evaluations.

Water knockout

After leaving the preheat cyclones (Figure 4), the hot calciner off-gas stream is used to superheat steam for power production as shown in Figure 5. Using data from Carbon Engineering's simulation, we found it to deliver 9 MW of heat to the superheater for an incoming temperature of 454°C and an outgoing temperature[3] of 325°C; using our own value of 448°C as the incoming temperature, we obtain an exit temperature of 319°C by energy balance for the same superheater heating rate. The cooled gas then passes through a knockout drum, where it is sprayed with incoming water to condense and remove a portion of its moisture before delivery to the intercooled compression system, while liquid water is diverted to wash $CaCO_3$ pellets before their arrival in the slaker.[3]

Figure 5 shows a general schematic of the water knockout system. For analysis purposes, we treat the knockout drum as adiabatic with two heat removal steps added: one for the gas stream to the compression system and the other for liquid

water to the pellet washer (labeled HR1 and HR2, respectively, in Figure 5). HR1 can serve to represent the cooling stage prior to the first compression stage, as is typical to minimize compression work via temperature and gas volume reduction,[16] where additional water is condensed and removed, presumably being diverted to the pellet washing station. This flow of condensed water is labeled $\dot{m}_{w,c}$, where its value and those of variables $\dot{m}_{v,c}$ (mass flow of vapor to the first compressor inlet) and T_c (flow temperature at first compressor inlet) depend on the heat removal rate $\dot{Q}_1$.

Although it is unclear from Carbon Engineering's paper[3] whether a specific water temperature is necessary for pellet washing, $\dot{Q}_2$ represents the heat removal rate associated with cooling the liquid water stream leaving the drum to T_{PW}, the temperature at which water arrives at the washing station. Thus, the total heat removed from the system is calculated simply as $\dot{Q}_r = \dot{Q}_1 + \dot{Q}_2$.

We model all components to operate at ambient pressure (1 bar), with the incoming water stream at ambient temperature (21°C). For simplicity, we ignore the dissolution of carbon dioxide, oxygen, or nitrogen in water. As a result, we find the knockout drum's internal temperature to be 60.5°C, where 17.9 t/h of water leaves as saturated vapor with the gas stream and 543.2 t/h leaves as liquid to the pellet washing station.

The plots of Figure 6 visualize how heat removal rate, work loss, vapor mass fraction, and water removal fraction relate to the temperature at the inlet of the first compressor stage (T_c). To produce the plots, we fix the washing station water temperature at T_{PW}=21°C, where we find $\dot{Q}_2$ = 24.9MW. Water removed (%) is calculated as the percentage change in water content of the knockout drum's incoming and outgoing gas flow.

Figure 6A shows that lower temperatures of the gas flow to the first compressor inlet correspond to lower water vapor content, while Figure 6B shows that to realize these lower temperatures, increasing amounts of cooling power are required. Therefore, if additional compression work due to vapor content is to be avoided, adequate cooling of the gas stream leaving the knockout drum is a necessity.

We find the superheater/knockout drum system's maximum work loss to be

$$\dot{W}_{\text{loss}}^{WK} = 7.8\ \text{MW}\ \left(3.1\%\ \text{of}\ \dot{W}_{\text{loss}}^{NG}\right),$$

equal in value to the maximum available work associated with bringing the superheater's outgoing stream from 319°C to the temperature of the surrounding environment (21°C). It should be noted that lower values of work loss in Figure 6B do not necessarily imply improvement to the second-law efficiency of the plant as a whole—they simply reflect differences in thermomechanical work potential between the water knockout system's incoming and outgoing flows. Because lower work loss in the knockout system implies higher outgoing temperature T_c and vapor content for the CO_2 stream, the intercooled compression system's power and cooling requirements would increase as a result.[16] Thus, improvements to the water knockout system would recover up to 7.8 MW of work or 37.8 MW of medium-grade process heat from the 319°C CO_2 stream prior to its arrival in the knockout drum, thereby minimizing heat removal requirements for optimal compressor inlet conditions. For all flows exiting the system (Figure 5) at 21°C, we find an additional 12.9 MW of heat removal to be required prior to the first compressor stage to minimize the CO_2 stream's water vapor content to 1.03%.

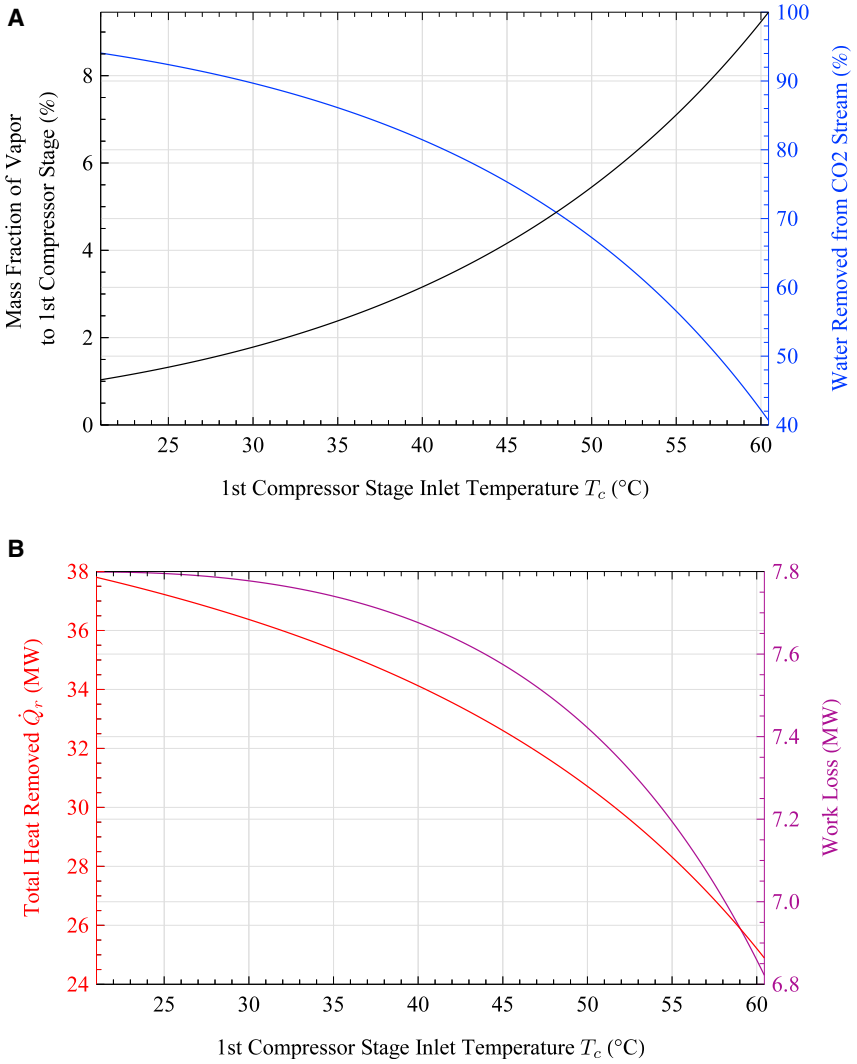

Figure 6. Selected water knockout data as functions of flow temperature at first compressor inlet (T_{PW}=21°C)

(A) Vapor mass fraction and water removal fraction.

(B) Heat removal rate and work loss.

CO_2 compression system

The reversible work requirement for isothermal compression of a pure CO_2 stream (111.9 t/h) is 6.74 MW for a delivery pressure of 151 bar. Accounting for additional CO_2 from natural gas combustion in the calciner and gas turbine (54.1 t/h for a total 166 t/h output CO_2 stream, Figure 5), the isothermal reversible work requirement becomes ~10.0 MW.

The use of an idealized four-stage compression unit with intercooling, where pure CO_2 is cooled to T_0=21°C after each isentropic, adiabatic compression stage, we find the minimum reversible work requirement to be 12.2 MW, i.e., an additional 2.2 MW being required compared with the isothermal case, with pressure ratios of 4.43, 3.96, 3.30, and 2.57, respectively, for each compression stage. These pressure ratios result from particle swarm optimization to minimize total reversible work as a function of intermediate pressures p_1, p_2, and p_3, where initial pressure p_0 =

101.325kPa and final pressure $p_4 = 15100$ kPa were fixed, and no intercooling pressure drop was assumed. Properties were calculated based on Span and Wagner's equation of state[17] for CO_2.

Here we do not include the influence of O_2, N_2, and H_2O due to the difficulty in predicting the quaternary mixture's thermodynamic behavior outside of the ideal gas region. Van Wagener[18] considers multi-stage compression of a CO_2/saturated vapor mixture. Using the same data in our calculations as in Van Wagener[18], we find a <1.6% difference in final work estimates; hence, we deem our work estimate reasonable owing to the large mass fraction of CO_2 (>97%).

In this case, with CO_2 transitioning to the liquid phase at 21°C, 58.66 bar, the fourth compressor would act as a pump for a portion of the process. In practice, it may be necessary to ensure that the CO_2 maintains a vaporous or supercritical state to avoid equipment complications.

Carbon Engineering gives a 22 MW power requirement for their compression system.[3] Thus, the 12.2 MW reversible work value gives an irreversible loss of

$$\dot{W}_{\text{loss}}^{\text{comp}} = 9.8\ \text{MW}\ \left(3.9\%\ \text{of}\ \dot{W}_{\text{loss}}^{NG}\right).$$

A significant portion of compression work is dedicated to processing CO_2 from natural gas combustion. Using Carbon Engineering's compressor power estimate[3] of 132 kWh/t-CO_2, the 54.1 t-CO_2/h produced by gas combustion between the CCGT power island and the calciner corresponds to an additional 7.1 MW of compressor power demand (or 32% of its total 22 MW power demand). This value becomes 4.0 MW for reversible four-stage compression, or 3.3 MW for isothermal compression.

Indeed, the handling of CO_2 produced by natural gas is critical for the plant to maintain its net-negative credentials, although it lends credence to the argument that the use of hydrocarbon fuels for a carbon-removal installation is counterproductive. In the context of energy use, it is clear that energy savings may be realized by eliminating the use of natural gas, primarily in the calciner, in which it plays its most dominant role. In addition, integration of intercooling stages with a preheat system for steam-cycle feedwater (namely, for the slaker and steam turbine system) may be a productive route to explore. This concept and its potential for energy savings is discussed in detail by Romeo et al.[16]

Power island

In the plant's A configuration, a CCGT power plant is used to produce power for all components, where a GE LM2500 DLE combined-cycle 2 × 1 system is used.[3,19] While in practice, the system's steam turbine will consume steam from both the slaker and the CCGT system's heat recovery steam generator, Carbon Engineering models steam cycles for the slaker (9.8 MW of power produced) and the CCGT system (46 MW of power produced) independently for simplicity.[3] Using this modeling procedure, determination of irreversible losses is also made relatively simple.

The CCGT power plant's loss to irreversibilities is easily determined by considering the work potential of its fuel. Using the reported rate of CH_4 consumption,[3] that is, 6.3 t/h, with the Gibbs free energy of reaction $\triangle \overline{g}_R(294\ \text{K}, 1\ \text{atm}) = -800.8$ kJ/mol, the fuel's work potential is 87.5 MW, i.e., the CCGT system sees a loss of

$$\dot{W}_{loss}^{CCGT} = 41.5\ \text{MW}(16.4\%\ \text{of}\ \dot{W}_{loss}^{NG})$$

to irreversibilities, given its 46 MW net power production. The fuel's work potential may also be found by dividing the 46 MW produced by General Electric's published efficiency value (52.9%) for the 60 Hz, 2 × 1 configuration in question.[19]

Using the mass flow and the state of post-superheat slaker steam provided by Carbon Engineering (70.2 t/h at 415°C, 4.2 MPa)[3] in combination with their condenser's operating temperature of 50°C, we find that a fully reversible, adiabatic (i.e., isentropic) turbine would produce 20.8 MW of power with a vapor quality of 83% at its exit. Thus, with 9.8 MW of reported power production, the steam turbine contributes an irreversible loss of

$$\dot{W}_{loss}^{ST} = 11\ \text{MW}\ (4.4\%\ \text{of}\ \dot{W}_{loss}^{NG}).$$

Chemical exergy dissipation (external to calciner) and other losses

The keen observer will notice that, while natural gas provides 186 MW of work potential to the calciner, only 63 MW of this potential is destroyed within its system boundaries. Hence, ~123 MW of work potential leaves the calciner with the outgoing flows, where ~24 MW leaves as thermomechanical exergy to the steam superheater (CO_2, O_2, N_2, H_2O at 448°C, ~13.5 MW) and slaker (CaO at 677°C, ~10.8 MW).

The remaining 99 MW provided by natural gas is stored as chemical exergy, which in fact is almost entirely attributable to the Gibbs free energy of reaction for $CaCO_3$ decomposition at T_0:

$$CaCO_3 \rightarrow CO_{2(g)} + CaO : \triangle \overline{g}_R(294\ \text{K},\ 1\ \text{bar}) = 131.9\ \text{kJ/mol},$$

with 294 t/h of $CaCO_3$ undergoing reaction.

This exergy, in principle, could be converted to useful work downstream, although this is not done in the process as presented. Instead, farther downstream, the vast majority of this chemical exergy is released as heat of reaction[3] in the slaker, pellet reactor, and air contactor, with respective chemical reactions:

$$CaO + H_2O \rightarrow Ca(OH)_2 : \triangle \overline{h}_R = -63.9\ \text{kJ/mol},$$

$$K_2CO_3 + Ca(OH)_2 \rightarrow 2KOH + CaCO_3 : \triangle \overline{h}_R = -5.8\ \text{kJ/mol},$$

$$CO_{2(g)} + 2KOH_{(aq)} \rightarrow H_2O_{(l)} + K_2CO_{3(aq)} : \triangle \overline{h}_R = -95.8\text{kJ/mol}.$$

Due to the relatively small heat of reaction, the loss in the pellet reactor is of less importance, where 5.7 MW of heat is released for a 0.979 kmol/s $Ca(OH)_2$ flow in solution. A portion of the heat released in the slaker, which is 52.2 MW for a 165 t/h CaO flow, contributes to steam generation for the turbine, recovering 9.8 MW of work potential, and as process heat for feedwater (see the lime cooler).[3]

The exothermic reaction in the air contactor releases 67.7 MW of heat for 111.9 t/h CO_2 captured. However, because air and KOH solution flow through the air contactor in such massive volumes, the reaction heat released imparts a negligible temperature change in them. While the air passing over the sorbent material is indeed cooled by evaporative cooling from the KOH solution, due to the reaction heat released, the cooling effect is slightly reduced. Overall, because the stored chemical

exergy of natural gas is freed here at low temperature, no work recovery is possible, as can be seen in the second term of Equation (4).

Thus, one may argue that losses from the calciner far exceed the 63 MW for the process within the boundaries of the calciner system (Figure 4). Indeed, the large (endothermic) heat of reaction demanded for decomposition of $CaCO_3$ leads not only to the calciner's high temperature requirement (>890°C) and corresponding losses in heat transfer, but also to a large amount of stored chemical exergy in CaO, which can then be only partly recovered, it being largely dissipated as low-grade heat into the environment via the air contactor. Therefore, the excessive energy required to recover CO_2 from $CaCO_3$ may be argued to be the chief driving factor behind large irreversible losses in Carbon Engineering's plant.

The large amount of air that must be moved through the air contactor requires a significant amount of power (9.2 MW)[3] to drive the fans. Based on our formulation of the system, i.e., with respect to thermodynamic separation work, we consider this to be a total loss (3.7% of $\dot{W}_{loss}^{NG}$).

While we do not analyze the chemical mechanisms for chemical exergy dissipation in the slaker, pellet reactor, and air contactor in detail, when considering the net work loss with respect to energy consumed $\dot{W}_{loss}^{NG} = 252$ MW, with 152.7 MW accounted for, the remaining loss of work potential to irreversibilities becomes:

$$\dot{W}_{\text{loss}}^{\text{chem + other}} = 99.3 \text{ MW } (39.4\% \text{ of } \dot{W}_{\text{loss}}^{NG}).$$

Summary of major losses

Carbon Engineering's proposed DAC plant removes 111.9 t-CO_2/h from ambient air while consuming 273.2 MW of work potential from natural gas. As mentioned before, the thermodynamically required minimum, i.e., reversible, work for separation and compression for this process is $\dot{W}_{\text{rev}}^{\text{tot}} = 21.20$ MW. Hence, a total loss of $\dot{W}_{\text{loss}}^{NG} = 252$ MW occurs due to irreversibilities in the various subprocesses of the DAC system, or a loss of $\dot{W}_{\text{loss}}^{\text{tot}} = 258$ MW when accounting for evaporation of water in the air contactor. Table 1 summarizes these losses.

Natural gas use in the calciner

We account for 152.7 MW of irreversible losses by detailed analysis of individual components, viz. the calciner, CCGT system, steam turbine, ASU, compression system, and water knockout, with the contactor fans' power requirement (9.2 MW) being considered a total loss. The remaining 99.3 MW of losses are attributable to the combined effects of uncontrolled chemical reactions and thermal dissipation in the air contactor, pellet reactor, and slaker.

In the A configuration studied, all energy, and hence exergy, supply is through natural gas, with 186 MW fed directly to the calciner and 87 MW fed to the power island. With 92.4% of incoming exergy lost to irreversibilities, we can state that the largest irreversible losses are attributable to exergy dissipation in exothermic chemical reactions, the second largest occurring within the calciner itself. Based on our analysis, we find an overall second-law efficiency of 7.8% for Carbon Engineering's plant based on a minimum (reversible) work requirement of 21.20 MW.

The 186 MW of energy entering the calciner, provided via natural gas, is mostly used to drive the endothermic calcium carbonate reaction ($CaCO_{3(s)} \rightarrow CaO_{(s)} + CO_{2(g)}$). However, some is consumed in heating incoming solids and combustion products

(CO_2, H_2O) to the calciner's operating temperature (1,173 K), as is required for reaction equilibrium. The calculated 63 MW work loss in the calciner is mainly due to devaluation of the natural gas—which has a work potential close to its heat of reaction[9]—by combustion into a very hot product and subsequent heat transfer into the hot solid (CaO) outflow, where irreversible mixing of flows and entropy generation through the uncontrolled chemical reaction are also significant contributors.

In addition to the largely unavoidable irreversible losses associated with its use as a calciner feedstock, the use of natural gas as an energy source for liquid-sorbent DAC processes bears further discussion for a variety of reasons:

- Natural gas is non-renewable; hence, a resource of finite supply must be exploited for a relatively inefficient process. If natural gas is to be involved as an energy source for DAC, its usage should be restricted only to those applications that cannot be powered by other means.
- For each ton of CO_2 removed from air, the use of natural gas adds $\sim \frac{1}{2}$ ton of CO_2 from combustion. This not only increases the compressors' power requirements by ~50%, but also necessitates ~50% larger cavities (or 50% larger volumes of reactive rock)[20] for long-term CO_2 storage. If the use of DAC increases in the future, so will the value of suitable space for permanent storage, space that should not be unnecessarily occupied by CO_2 produced within the capture process itself.
- If DAC is to be implemented on a meaningful scale with respect to IPCC removal rate targets,[1] exclusive use of natural-gas-driven processes such as Carbon Engineering's A configuration with its determined second-law efficiency will require over half of the world's current natural gas production,[8] likely increasing the price of the commodity unless its production increases proportionally.
- One could argue, however, that if natural gas is to be used substantially in the future, it should be used in processes such as DAC that allow for capture and storage of the resulting CO_2, although its use for power generation with carbon capture and storage may be more productive.

While the more minor losses between the water knockout and the compression systems may be partially avoided if natural gas use is curbed, we also note that if natural gas use persists, the water knockout system in particular presents the opportunity to recover up to 37.8 MW of medium-grade process heat from the gas stream leaving the superheater, equivalent to 7.8 MW in work potential. A simple steam cycle may harness at least some of this potential to power smaller components or auxiliary systems (requiring 2.6 MW in total).[3]

Renewable energy use

For sustainable operation of DAC processes, the use of renewable energy sources as substitutes for natural gas must be considered. While we leave the proposal and detailed analysis of alternative configurations to the future, we briefly estimate the possible impacts:

The power required to drive the Carbon Engineering process is partly obtained through heat recovery from exothermic chemical reactions, although most power is derived from combustion of natural gas in the gas turbine(s). Replacing natural gas use with renewable energy sources, such as wind, solar, etc., will require, at minimum, some modifications to the system's management of process heat.

The use of renewable energy for the calciner may be possible, two options being direct electrical heating or replacing natural gas with green hydrogen (i.e., electrolysis of water using electricity provided from renewable sources), barring considerations of land use, energy storage to accompany the method of renewable power production, and other technical risks. Likewise, the CCGT power island may also be replaced, provided enough renewable capacity is installed; doing so would avoid 17.3 t-CO_2/h from combustion being introduced into the plant for processing, reducing necessary $CaCO_3$ production by 39 t/h.

With an electrolyzer splitting water into stoichiometric amounts of fuel (H_2) and oxidizer (O_2), and with electrical heating requiring no combustion, both modifications would eliminate the need to provide an oxygen stream for oxy-fuel combustion in the calciner. Hence, in both scenarios, the ASU is removed, reducing the power requirement by 13.3 MW. At the same time, the additional 54.1 t-CO_2/h produced from natural gas combustion in the calciner and CCGT unit is eliminated from the calciner's product stream, reducing the compression system's power requirement by ~7.1 MW (~32%).

By these estimates, the use of renewable energy for power and calciner heat would reduce the plant's mechanical power demand (between the ASU and the compressors) by ~20.4 MW.

Assuming green hydrogen to be used in the calciner and the CCGT system to be replaced with renewable power, processing 111.9 t/h of CO_2 captured from the atmosphere would require an ~261 t/h flow of $CaCO_3$, reducing the calciner's thermal energy requirement to ~162 MW (estimated at 3.18 GJ/t-CaO with 78% thermal efficiency, assuming that 6.0 t-$CaCO_3$/h is rejected back to the pellet reactor[3]). The use of hydrogen combustion ($2H_2 + O_2 \rightarrow 2H_2O$: $\triangle \overline{h}_R = -241.8$ kJ/mol) to meet this demand would require a feed of 4.86 t/h H_2, or 53,892 Nm^3-H_2/h, and 38.5 t/h O_2 (both produced via electrolysis). Likewise, the gas flow leaving would consist of 43.3 t/h H_2O and 111.9 t/h CO_2, a total flow of ~155 t/h as opposed to 201 t/h from the natural gas configuration (Figure 4).

For a commercially available electrolyzer, we selected Thyssenkrupp's advanced alkaline water electrolyzer modules, their "20 MW" module producing 4,000 Nm^3-H_2/h with a DC power consumption of 4.3 kWh/Nm^3, and their "10 MW" module producing 2,000 Nm^3-H_2/h for the same DC power consumption.[21] To produce the 53,892 Nm^3/h demanded by the new calciner, thirteen 20 MW units and one 10 MW unit may be used, resulting in ~232 MW of DC power required for the electrolyzer stack, along with an added flow of 54 t/h of water. Additional water knockout capacity would also be required to accommodate the added 13.2 t/h of water produced as a combustion product.

Finally, assuming all other plant components to demand the same amount of power as in the A configuration,[3] and accounting for the compressors' reduced power requirements and elimination of the ASU and CCGT CO_2 absorber, an additional 35 MW of renewable power would be required to replace the previous CCGT power island.

Thus, by these very simplified estimates, the use of a green hydrogen-fired calciner and a renewable power island would reduce overall energy demand to roughly 232 MW + 35 MW = 267 MW of renewable electrical energy, assuming no inverter losses for the power island. This corresponds to a 2.2% decrease compared with the natural gas configuration demanding 273.2 MW, where a portion of work losses would now

be due to the inefficiencies of electrical-to-chemical energy conversion in the electrolyzer. The question therefore remains whether any benefits of this configuration, namely, reduced CO_2 storage space requirements, are worth their cost, i.e., the purchase and maintenance of large electrolyzer stacks and installation of enough renewable capacity to reliably provide 267 MW of power with the necessary electrical and hydrogen storage.

We leave to future work a detailed comparison to the natural gas configuration, which, during a period of global energy system transition, may be the better choice.

With the calciner being directly heated via electricity, and with the power island being replaced with only renewable capacity as discussed above, there would be no combustion products and hence no losses to mixing of gas flows nor additional heat/power requirements for these products' processing. With the same reduction of 20.4 MW for the ASU and compression system, and again considering the calciner's thermal demand to be 162 MW, with the remaining power demand totaling 35 MW, we estimate the plant's net energy consumption to be 162 MW + 35 MW = 197 MW, where all electrical power input to the calciner is released as heat.

Thus, on the basis of energy consumption, an all-electric plant configuration would likely be the ideal option to pursue. However, use of electric heating for the calciner begs the question of how $CaCO_3$ pellets are to be fluidized, possibly using a flow of recirculating CO_2, and the energy inputs required for this fluidization system.

Regardless of how heat is provided, though, a minimum of $q_{calc}^{min} = 1.66 \frac{GJ}{t-CaCO_3}$ will always be required to sustain the decomposition of $CaCO_3$, given its enthalpy of reaction,

$$\triangle \overline{h}_R(900^\circ C, 1\ bar) = 166.2 kJ/mol,$$

or $\dot{Q}_{calc}^{min} = 117 MW$ for a 261 t/h flow of $CaCO_3$ with 6 t/h not consumed. Given this minimum amount of heat, for electrical heating we estimate the minimum entropy generation as:[9]

$$\dot{S}_{gen} = \frac{\dot{Q}_{calc}^{min}}{T_H} = \frac{\dot{W}_{elec}^{min}}{T_H},$$

and hence the minimum work loss as:

$$\dot{W}_{loss}^{min} = T_0 \dot{S}_{gen} = \frac{T_0}{T_H} \dot{W}_{elec}^{min} = 29.3\ MW,$$

where T_H = 1,173 K is the calciner's operating temperature. More detailed analysis and discussion of an all-electric calciner is available in Long-Innes.[15]

We also note that an all-electric plant configuration may be difficult to realize in practice, primarily owing to the difficulty of efficiently providing process heat at 900°C to the calciner. The massive installed capacity of intermittent renewables such as solar and wind must also be taken into account.

For the full plant, including an electric calciner, to be powered by renewables, McQueen et al.[22] estimate requirements of between 750 and 1,100 MW of installed solar capacity with 4,400 to 5,100 MWh of battery storage, or 500 MW of installed wind capacity with 3,200 MWh of battery storage, both of which have significant cost implications. By their estimates, nuclear and geothermal power tie for the lowest installed capacity of 240 MW (given nine DAC plants being powered by a

2,200 MW nuclear facility).[22] Logically, these requirements would be even larger for the hydrogen configuration discussed earlier.

It will also be necessary to examine improvements or pitfalls that may be realized downstream of the calciner by eliminating natural gas use, particularly with regard to internal power generation from heat released throughout the system (i.e., decreasing the degree of steam superheat due to the calciner products' reduced mass flow and/or heat capacity, Figure 5).

Losses of chemical exergy external to the calciner

In the natural gas configuration, the material leaving the calciner carries ~124 MW of chemical and thermomechanical exergy. As discussed earlier, the chemical exergy is released in the exothermic reactions in the slaker, pellet reactor, and air contactor. In the last, 67.7 MW of heat of reaction is dissipated into the passing air, which, independent of the primary energy source, remains irretrievable.

While quantities of heat released by each chemical reaction are easily determined, accurate accounting of unharvested chemical and thermomechanical exergy was not performed as part of this analysis. Thus, future work must analyze the slaker, pellet reactor, and air contactor components in detail to paint a clearer picture of the dissipation of exergy downstream of the calciner, i.e., the extent to which it is used for CO_2 separation, recovered as work, or irretrievably lost to the environment. Once these studies are performed, process improvements may be proposed that would ideally further reduce the plant's energy consumption in a cost-effective manner.

Irreversibility, efficiency and global impact

Carbon Engineering's DAC system as presented in Keith et al.[3] relies on natural gas as an energy source and requires ~13 times the thermodynamic minimum energy supply. In other words, only ~8% of the energy supply is used for the actual task of separating CO_2 from the air, while the remaining 92% is consumed by irreversible processes throughout the system. Our thermodynamic analysis aims to give insight into the major locations and causes of these losses, which we regard as an important step for development of improved alternative processes.

The most significant losses are attributed to the chemical steps within the system, where high temperature and large heat of reaction in the endothermic calciner reaction, coupled with the impossibility of energy recovery in the air contactor's exothermic reaction, result in unavoidably high energy demand. Reduction of the associated losses appears to be impossible for the present reactions, which, however, are feasible, and work well. Alternative chemical cycles may reduce these losses.

Our simplified estimates show that the use of renewable energy with an electrically heated calciner may reduce the energy requirements of Carbon Engineering's DAC process, where we estimate a 20.4 MW reduction in power requirements due to elimination of the ASU and a smaller mass flow being processed by the compression system, and a 24 MW reduction in the calciner's thermal demand due to a reduced $CaCO_3$ input. These benefits, however, may be outweighed by the financial costs of installing and maintaining the required renewable capacity.[22]

With a single, all-electric plant consuming a minimum of 197 MW to remove 111.9 t-CO_2/h at a high capacity factor (>0.90), removal of 10 Gt-CO_2/year would require at least 11,335 plants, consuming in total 2.23 TW, or 19,534 TWh/year, of renewable electricity—roughly 73% of current global electricity generation by all means (26,619

TWh/year).[8] For the same 10 Gt/year removal rate, Carbon Engineering's natural gas-driven DAC process would require 58% of 2019's global natural gas production.[8]

The task of direct air capture (DAC) of CO_2 at rates significant enough to have a global impact (10 Gt/year) is tremendous, where even fully reversible systems would require large portions of the world's current power generation or natural gas production. At the desired rates of CO_2 removal,[1] the use of DAC systems would have a significant impact on the world's energy systems. It goes without saying that if DAC is to have a meaningful future, substantial improvements in process design and efficiency are vital.

EXPERIMENTAL PROCEDURES

Resource availability

Lead contact

The lead contact is Henning Struchtrup (struchtr@uvic.ca).

Materials availability

This study did not generate new unique materials.

Data and code availability

All data needed to evaluate the conclusions in the paper are presented in the paper and its supplemental information. Additional data related to this paper may be requested from the authors.

Methods

Wolfram Mathematica and MathWorks' MATLAB software were used to solve the equations because they keep track of all variables in use, computed outflows from one subsystem are applied as inflows to another, and a general picture of energy consumption and subsystems' losses to irreversibilities can be obtained without the use of specialized simulation software.

Shomate equations were used to calculate the majority of heat capacity and enthalpy and entropy values used in MATLAB and Mathematica, their use being deemed sufficiently accurate when the ideal gas equation was satisfied to at least 95% accuracy (i.e., for any species in question, $pv/RT>0.95$). All Shomate constants and other thermochemical data (molar masses, standard enthalpies, standard entropies) were obtained from the NIST Chemistry WebBook,[23] with the exception of $CaCO_3$, where published data by Jacobs et al.[24] was used, and water vapor <500 K, whose Shomate constants were obtained from Cengel and Boles.[25] The enthalpy reference point for all chemical species was chosen as their enthalpy of formation at standard conditions (1 bar, 298.15 K); see Note S3 for details.

Where Shomate equations/ideal gas assumptions were not sufficiently accurate ($pv/RT<0.95$), or when water occurred in a liquid state, thermophysical properties were calculated from a MATLAB implementation of the IAPWS IF-97 standard[26] for water and steam, while CO_2 properties at high pressures were calculated from a similar implementation of Span and Wagner's equation of state[17] for CO_2.

SUPPLEMENTAL INFORMATION

Supplemental information can be found online at https://doi.org/10.1016/j.xcrp.2022.100791.

ACKNOWLEDGMENTS

We gratefully acknowledge support from the National Science and Engineering Research Council of Canada (NSERC, grant RGPIN-2016-03679). We also thank the Pacific Institute for Climate Solutions (PICS), Ocean Networks Canada, and the Solid Carbon team for their valuable input.

AUTHOR CONTRIBUTIONS

Both authors collaborated closely and made equal overall contributions to the project. Specifically, H.S. devised the project, set up the model, and performed some evaluations. R.L.-I. expanded the modeling, performed most evaluations, and wrote the manuscript in consultation with H.S.

DECLARATION OF INTERESTS

The authors declare no competing interests.

Received: September 24, 2021
Revised: December 21, 2021
Accepted: February 8, 2022
Published: March 2, 2022

REFERENCES

1. Rogelj, J., Shindell, D., Jiang, K., Fifita, S., Forster, P., Ginzburg, V., Handa, C., Kheshgi, H., Kobayashi, S., Kriegler, E., et al. (2018). Global Warming of 1.5°C. An IPCC Special Report on the Impacts of Global Warming of 1.5°C above Pre-industrial Levels and Related Global Greenhouse Gas Emission Pathways, in the Context of Strengthening the Global Response to the Threat of Climate Change, Sustainable Development, and Efforts to Eradicate Poverty, IPCC Special Report (Intergovernmental Panel on Climate Change, Geneva). https://www.ipcc.ch/site/assets/uploads/sites/2/2019/05/SR15_Chapter2_Low_Res.pdf.

2. Osman, A.I., Hefny, M., Abdel Maksoud, M.I.A., Elgarahy, A.M., and Rooney, D.W. (2020). Recent advances in carbon capture storage and utilisation technologies: a review. Env. Chem. Lett. *19*, 797–849. https://doi.org/10.1007/s10311-020-01133-3.

3. Keith, D.W., Holmes, G., Angelo, D.S., and Heidel, K. (2018). A process for capturing CO2 from the atmosphere. Joule *2*, 1573–1594. https://doi.org/10.1016/j.joule.2018.05.006.

4. Paris Agreement to the United Nations Framework Convention on Climate Change (2016). United Nations treaty collection. https://unfccc.int/sites/default/files/english_paris_ agreement.pdf.

5. The National Academies of Sciences, Engineering and Medicine (2019). Negative Emissions Technologies and Reliable Sequestration: A Research Agenda (The National Academies Press, Washington, DC). https://doi.org/10.17226/25259. https://www.nap.edu/read/25259/.

6. TheWorld Bank, Consumer price index (2010 = 100) - United States. url: https://data.worldbank.org/indicator/FP.CPI.TOTL?locations=US

7. The World Bank, GDP (constant 2010 US$). url: https://data.worldbank.org/indicator/NY.GDP.MKTP.KD

8. IEA (2020). Key world energy statistics 2020. https://www.iea.org/reports/key-world-energy-statistics-2020.

9. Struchtrup, H. (2014). Thermodynamics and Energy Conversion, First Edition (Springer-Verlag). https://doi.org/10.1007/978-3-662-43715-5.

10. Dlugokencky, E.J., Mund, J.W., Crotwell, A.M., and Thoning, K.W. (2021). Atmospheric Carbon Dioxide Dry Air Mole Fractions from the NOAA GML Carbon Cycle Cooperative Global Air Sampling Network, 1968- 2020. https://doi.org/10.15138/wkgj-f215.

11. Herzog, H.J. (2001). What future for carbon capture and sequestration? Environ. Sci. Technol. *35*, 148–153. https://doi.org/10.1021/es012307j.

12. Caram, H.S., Gupta, R., Thomann, H., Ni, F., Weston, S.C., and Afeworki, M. (2020). A simple thermodynamic tool for assessing energy requirements for carbon capture using solid or liquid sorbents. Int. J. Greenhouse Gas Control *97*, 102986. https://doi.org/10.1016/j.ijggc.2020.102986.

13. McQueen, N., Gomes, K.V., McCormick, C., Blumanthal, K., Pisciotta, M., and Wilcox, J. (2021). A review of direct air capture (DAC): scaling up commercial technologies and innovating for the future. Prog. Energy *3*, 032001. https://doi.org/10.1088/2516-1083/abf1ce.

14. Sabatino, F., Grimm, A., Gallucci, F., Annaland, M.v.S., Kramer, G.J., and Gazzani, M. (2021). A comparative energy and costs assessment and optimization for direct air capture technologies. Joule *5*, 2047–2076. https://doi.org/10.1016/j.joule.2021.05.023.

15. Long-Innes, R. (2021). Thermodynamic Analysis of a Direct Air Carbon Capture Plant with Directions for Energy Efficiency Improvements, Master's thesis (University of Victoria). https://dspace.library.uvic.ca/handle/1828/13681.

16. Romeo, L.M., Bolea, I., Yolanda, L., and Escosa, J.M. (2009). Optimization of intercooling compression in CO2 capture systems. Appl. Therm. Eng. *29*, 1744–1751. https://doi.org/10.1016/j.applthermaleng.2008.08. 010.

17. Span, R., and Wagner, W. (1996). A new equation of state for carbon dioxide covering the fluid region from the triple-point temperature to 1100 K at pressures up to 800 MPa. J. Phys. Chem. Ref. Data *25*, 1509–1596. https://doi.org/10.1063/1.555991.

18. Van Wagener, D.H. (2011). Stripper Modeling for CO2 Removal Using Monoethanolamine and Piperazine Solvents, Doctoral dissertation (University of Texas). https://repositories.lib.utexas.edu/handle/2152/ETD-UT-2011-08-4302.

19. General Electric Company (2021). GEA34340 LM2500 Power Plants 60Hz FS. https://www.ge.com/content/dam/gepower-new/global/en_US/downloads/gas-new-site/products/gas-turbines/lm2500-60hz-fact-sheet-product-specifications.pdf.

20. Snæbjörnsdóttir, S.Ó., Sigfússon, B., Marieni, C., Goldberg, D., Gislason, S.R., and Oelkers, E.H. (2020). Carbon dioxide storage through mineral carbonation. Nat. Rev. Earth Environ. *1*, 90–102. https://doi.org/10.1038/s43017-019-0011-8.

21. Thyssenkrupp Industrial Solutions (2020). Hydrogen from large-scale electrolysis: efficient solutions for sustainable chemicals and energy storage. https://d2zo35mdb530wx.cloudfront.net/_binary/UCPthyssenkruppBAISUhdeChlorineEngineers/en/products/water-electrolysis-hydrogen-production/alkaline-

water-electrolysis/link-thyssenkrupp_Hydrogen_Water_ Electrolysis_and_green_chemicals.pdf.

22. McQueen, N., Desmond, M.J., Socolow, R.H., Psarras, P., and Wilcox, J. (2021). Natural gas vs. Electricity for solvent-based direct air capture. Front. Clim. *2*, 618644. https://doi.org/10.3389/fclim.2020.618644.

23. Linstrom, P.J., and Mallard, W.G. (1997). NIST Chemistry WebBook, NIST Standard Reference Database, *69* (National Institute of Standards and Technology). https://doi.org/10.18434/T4D303.

24. Jacobs, G.K., Kerrick, D.M., and Krupka, K.M. (1981). The high-temperature heat capacity of natural calcite (CaCO3). Phys. Chem. Minerals *7*, 55–59. https://doi.org/10.1007/BF00309451.

25. Cengel, Y., and Boles, M. (1997). Thermodynamics: An Engineering Approach, Ninth Edition (McGraw-Hill).

26. International Association for the Properties of Water and Steam (2007). Revised release on the IAPWS industrial formulation 1997 for the thermodynamic properties of water and steam. http://www.iapws.org/relguide/IF97-Rev.pdf.

Cell Reports Physical Science, Volume *3*

Supplemental information

Thermodynamic loss analysis of a liquid-sorbent direct air carbon capture plant

Ryan Long-Innes and Henning Struchtrup

Note S1: The Calciner and $CaCO_3$ Decomposition

As is argued in the main paper, the calciner's high thermal demand is largely unavoidable owing to $CaCO_3$'s high enthalpy of decomposition ($CaCO_{3\,(s)} \rightarrow CaO_{(s)} + CO_{2(g)}$, $\triangle \bar{h}_R = 179\,\mathrm{kJ/mol}$).

With no mixing entropies involved, as the decomposition yields only one gaseous species, the Law of Mass Action gives[1]

$$A = \sum_{\alpha} \gamma_\alpha \bar{g}_\alpha(T, p) = 0, \tag{S1}$$

i.e., affinity A vanishes in chemical equilbrium. Here, $\bar{g}_\alpha(T, p) = \bar{h}_\alpha(T, p) - T\bar{s}_\alpha(T, p)$ is species α's Gibbs Free Energy. γ_α is the same species' stoichiometric coefficient, being negative in sign if consumed by the reaction, and positive if produced. The reaction's equilibrium temperature as a function of pressure, obtained as the solution of Eq. (S1), is shown in Figure S1.

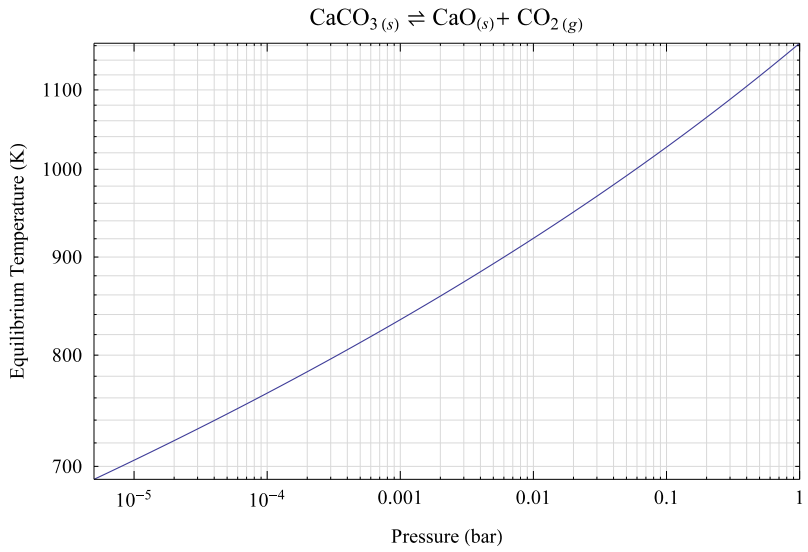

Figure S1: $CaCO_3$ Decomposition Reaction Equilibrium Temperature versus Pressure, Logarithmic Plot. For the existing design with calciner operation at an internal pressure of 1 bar, the equilibrium temperature is 1163 K (890°C), reducing by 45 K to 1118 K (845°C) with a 50% reduction of internal pressure, and more substantially by ∼136 K to 1027 K (754°C) for a 90% pressure reduction.

Overall, the calciner's required equilibrium temperature decreases as calciner pressure is reduced, though substantial decreases in temperature are only seen as internal pressure approaches a vacuum (Figure S1). The question therefore remains as to how pressure reduction to near-rarefied conditions may be accomplished in practice. One can speculate that the work required by pumps to maintain a vacuum would likely exceed any energy saved through marginally reducing the calciner's operating temperature, while the complexities of sealing such a system against atmospheric pressure would certainly increase technical risk and overall costs. Thus, operation outside of ambient pressure can safely be assumed to be a costly and impractical solution to reduce energy demand, hence our argument in the main paper that it would likely be an unproductive process improvement route to pursue.

Note S2: Application of Balance Equations to ASU

A sample calculation of the work loss for the Air Separation Unit (ASU) is performed to demonstate application of the balance equations of the main paper's 'Methods' section and the Shomate equations as described.

We begin by reiterating the balance equations of the main paper, namely, the mass balance, energy balance, entropy balance, and combined energy/entropy balance, written respectively as

$$\sum_{out} \dot{m}_e = \sum_{in} \dot{m}_i, \tag{S2}$$

$$\sum_{out} \dot{n}_e \bar{h}_e - \sum_{in} \dot{n}_i \bar{h}_i = \dot{Q}_0 + \sum_k \dot{Q}_k - \dot{W}, \tag{S3}$$

$$\sum_{out} \dot{n}_e \bar{s}_e - \sum_{in} \dot{n}_i \bar{s}_i - \frac{\dot{Q}_0}{T_0} - \sum_k \frac{\dot{Q}_k}{T_k} = \dot{S}_{gen} \geq 0, \tag{S4}$$

and

$$\dot{W} = -T_0 \dot{S}_{gen} + \sum_k (1 - \frac{T_0}{T_k}) \dot{Q}_k + \sum_{in} \dot{n}_i (\bar{h}_i - T_0 \bar{s}_i) - \sum_{out} \dot{n}_e (\bar{h}_e - T_0 \bar{s}_e). \tag{S5}$$

A component level diagram of the ASU is shown in Figure S2, with its system boundary at environmental temperature T_0 (21°C). We ask for the reversible work $\dot{W}_{rev}^{ASU}$ to separate the incoming air stream.

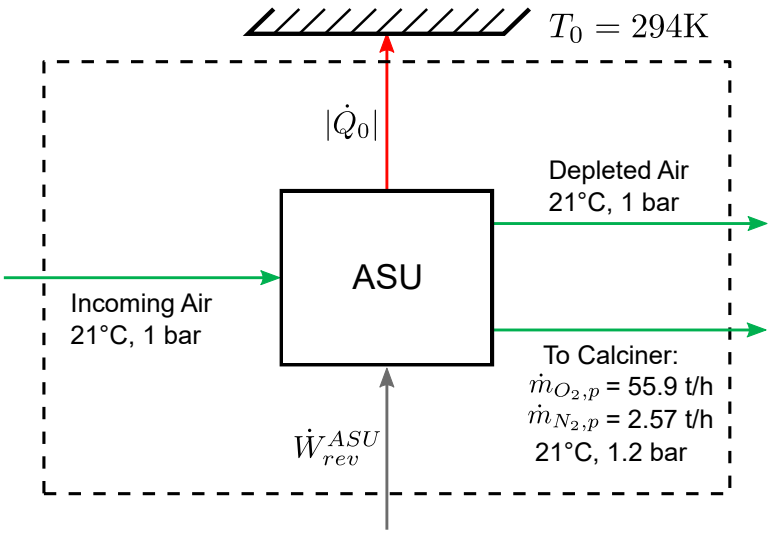

Figure S2: Air Separation Unit Component-Level Diagram. Based on Carbon Engineering's data, the ASU provides a 58.5 t/h flow to the calciner at 1.2 bar, with 95.60% of O_2, and 4.40% of N_2, see Ref. 2.

Mass Balance: We apply Eq. (S2) over the system of Figure S2 as

$$\dot{m}_d + \dot{m}_p = \dot{m}_i, \tag{S6}$$

where subscripts d, p, and i refer to the depleted air stream, the product stream (O_2 and N_2), and the incoming air stream, respectively.

Rewriting the mass balance for any component α gives

$$\dot{m}_{\alpha,d} + \dot{m}_{\alpha,p} = \dot{m}_{\alpha,i}, \tag{S7}$$

or by mole,

$$\dot{n}_{\alpha,d} + \dot{n}_{\alpha,p} = \dot{n}_{\alpha,i}. \tag{S8}$$

The mole fraction of component α is

$$X_{\alpha,k} = \frac{\dot{n}_{\alpha,k}}{\dot{n}_k}, \tag{S9}$$

where $\dot{n}_k$ is the sum of all component mole flows in gas stream k, with k being any of d, p, or i.

The component mole flows and mole fractions are easily determined for the outgoing stream, having known mass flows as shown in Figure S2. For the incoming air stream, we consider the same composition by mass as enters the Air Contactor[2] (0.060% CO_2, 23.00% O_2, 75.96% N_2 and 0.98% H_2O), and consider all O_2 to leave to the calciner, i.e.,

$$\dot{m}_{O_2,i} = \dot{m}_{O_2,p} = 55.93\,\mathrm{t/h}. \tag{S10}$$

From here, we determine the total incoming mass flow to be

$$\dot{m}_i = \frac{\dot{m}_{O_2,i}}{0.2300} = 243.2\,\mathrm{t/h} \tag{S11}$$

and solve for the remaining incoming quantities.

The same set of quantities are determined for the depleted air stream through application of Eq. (S7), completing the set of values as listed in Table S1.

Table S1: Mass Flows, Mole Flows and Mole Fractions for ASU Analysis

α	Product Stream to Calciner			Incoming Air			Depleted Air		
	$\dot{m}_{\alpha,p}\ (\frac{\mathrm{t}}{\mathrm{h}})$	$\dot{n}_{\alpha,p}\ (\frac{\mathrm{kmol}}{\mathrm{s}})$	$X_{\alpha,p}$	$\dot{m}_{\alpha,i}\ (\frac{\mathrm{t}}{\mathrm{h}})$	$\dot{n}_{\alpha,i}\ (\frac{\mathrm{kmol}}{\mathrm{s}})$	$X_{\alpha,i}$	$\dot{m}_{\alpha,d}\ (\frac{\mathrm{t}}{\mathrm{h}})$	$\dot{n}_{\alpha,d}\ (\frac{\mathrm{kmol}}{\mathrm{s}})$	$X_{\alpha,d}$
O_2	55.93	0.4855	0.9501	55.93	0.4855	0.2062	0	0	0
N_2	2.574	0.02552	0.04994	184.7	1.831	0.7778	182.1	1.806	0.9796
CO_2	0	0	0	0.1459	9.208e-4	3.910e-4	0.1459	9.208e-4	4.995e-4
H_2O	0	0	0	2.383	0.03674	0.01560	2.383	0.03674	0.01993

Energy and Entropy Balance: With our interest being in the reversible work/power to separate the incoming air stream, the $-T_0\dot{S}_{gen}$ term is eliminated from Eq. (S5), as is the $\sum_k(1-\frac{T_0}{T_k})\dot{Q}_k$ term due to no heat exchange taking place besides that with the environment ($\dot{Q}_0$). Thus, we rewrite the balance equation as

$$\dot{W}^{ASU}_{rev} = \sum_{in}\dot{n}_i(\bar{h}_i - T_0\bar{s}_i) - \sum_{out}\dot{n}_e(\bar{h}_e - T_0\bar{s}_e), \tag{S12}$$

where

$$\begin{aligned}\sum_{in}\dot{n}_i(\bar{h}_i - T_0\bar{s}_i) = {} & \dot{n}_{CO_2,i}\left[\bar{h}_{CO_2}(T_0) - T_0\left(\bar{s}^0_{CO_2}(T_0) - \bar{R}\ln(X_{CO_2,i})\right)\right] \\ & + \dot{n}_{O_2,i}\left[\bar{h}_{O_2}(T_0) - T_0\left(\bar{s}^0_{O_2}(T_0) - \bar{R}\ln(X_{O_2,i})\right)\right] \\ & + \dot{n}_{N_2,i}\left[\bar{h}_{N_2}(T_0) - T_0\left(\bar{s}^0_{N_2}(T_0) - \bar{R}\ln(X_{N_2,i})\right)\right] \\ & + \dot{n}_{H_2O,i}\left[\bar{h}_{H_2O}(T_0) - T_0\left(\bar{s}^0_{H_2O}(T_0) - \bar{R}\ln(X_{H_2O,i})\right)\right]\end{aligned} \tag{S13}$$

and

$$\begin{aligned}\sum_{out}\dot{n}_e(\bar{h}_e - T_0\bar{s}_e) = {} & \dot{n}_{O_2,p}\left[\bar{h}_{O_2}(T_0) - T_0\left(\bar{s}^0_{O_2}(T_0) - \bar{R}\ln(X_{O_2,p}) - \bar{R}\ln(1.2)\right)\right] \\ & + \dot{n}_{N_2,p}\left[\bar{h}_{N_2}(T_0) - T_0\left(\bar{s}^0_{N_2}(T_0) - \bar{R}\ln(X_{N_2,p}) - \bar{R}\ln(1.2)\right)\right] \\ & + \dot{n}_{CO_2,d}\left[\bar{h}_{CO_2}(T_0) - T_0\left(\bar{s}^0_{CO_2}(T_0) - \bar{R}\ln(X_{CO_2,d})\right)\right] \\ & + \dot{n}_{O_2,d}\left[\bar{h}_{O_2}(T_0) - T_0\left(\bar{s}^0_{O_2}(T_0) - \bar{R}\ln(X_{O_2,d})\right)\right] \\ & + \dot{n}_{N_2,d}\left[\bar{h}_{N_2}(T_0) - T_0\left(\bar{s}^0_{N_2}(T_0) - \bar{R}\ln(X_{N_2,d})\right)\right] \\ & + \dot{n}_{H_2O,d}\left[\bar{h}_{H_2O}(T_0) - T_0\left(\bar{s}^0_{H_2O}(T_0) - \bar{R}\ln(X_{H_2O,d})\right)\right].\end{aligned} \tag{S14}$$

Computed values of $\bar{h}_\alpha(T_0)$ and $\bar{s}^0_\alpha(T_0)$ as they pertain to Eqs. (S13) and (S14) are presented in Table S2, where environmental temperature $T_0 = 294\,\mathrm{K}$. All other quantities are available in Table S1.

Table S2: Values of $\bar{h}_\alpha(T_0)$ and $\bar{s}^0_\alpha(T_0)$ as they pertain to Eqs. (S13) and (S14)

α	$\bar{h}_\alpha(T_0 = 294\mathrm{K})\left(\frac{\mathrm{kJ}}{\mathrm{kmol}}\right)$	$\bar{s}^0_\alpha(T_0 = 294\,\mathrm{K})\left(\frac{\mathrm{kJ}}{\mathrm{kmol\,K}}\right)$
O_2	-117.490	204.753
N_2	-116.491	191.217
CO_2	-393,670	213.290
H_2O	-241,953	188.386

With all necessary quantities determined, evaluating Eq. (S12) gives

$$\dot{W}^{ASU}_{rev} = -2.895\,\mathrm{MW},$$

where its negative sign represents power being *consumed* by the component, as is expected. Finally, the work loss to irreversibilities is obtained by considering its reversible power consumption against its actual power consumption of 13.3 MW, i.e.,

$$\dot{W}^{ASU}_{loss} = \dot{W}^{ASU}_{rev} - \dot{W}^{ASU}_{act} = -2.985\,\mathrm{MW} - (-13.3\,\mathrm{MW}) = 10.4\,\mathrm{MW}$$

as is presented in the main paper.

Note S3: Shomate Equations

Shomate equations were used to determine the majority of thermophysical properties involved in the main paper's analyses. They were applied for gaseous species when the ideal gas law was satisfied to at least 95% accuracy, i.e., pv/RT > 0.95 (Table), as well as for solid species CaO, K_2CO_3 and $CaCO_3$. All Shomate constants were obtained from NIST,[3] with the exception of those for $CaCO_3$, found in Ref. 4, and those for water vapor $< 500\,\mathrm{K}$, found in Ref. 5.

With any ideal gas' molar specific internal energy $\bar{u}$ and enthalpy $\bar{h} = \bar{u} + p\bar{v} = \bar{u} + \bar{R}T$ depending only on temperature, the Shomate equation for its molar specific heat at constant pressure is also only a function of temperature:[1]

$$\bar{c}_p(T) = A + BT + CT^2 + DT^3 + \frac{E}{T^2}. \tag{S15}$$

Integration of $\bar{c}_p(T)$ gives enthalpy,

$$\bar{h}(T) = \int_{T_R}^{T} \bar{c}_p(T')dT' + \bar{h}^0_f, \tag{S16}$$

where $\bar{h}^0_f$ is the chemical species' enthalpy of formation at standard conditions ($T_R = 298.15\,\mathrm{K}$, $p_R = 1\,\mathrm{bar}$).

Evaluating Eq. (S16) gives the complete Shomate expression for molar specific enthalpy,

$$\bar{h}(T) = A(T - T_R) + B\frac{T^2 - {T_R}^2}{2} + C\frac{T^3 - {T_R}^3}{3} + D\frac{T^4 - {T_R}^4}{4} - E\left(\frac{1}{T} - \frac{1}{T_R}\right) + \bar{h}^0_f, \tag{S17}$$

as was implemented in Mathematica and MATLAB using the constants presented in Tables and S4.

The entropy of the ideal gas is

$$\bar{s}(T, p) = \bar{s}^0(T) - \bar{R}\ln(\frac{p}{p_R}), \tag{S18}$$

or, for component α in a mixture with mole fraction X_α,

$$\bar{s}_\alpha(T, p) = \bar{s}^0_\alpha(T) - \bar{R}\ln(X_\alpha) - \bar{R}\ln(\frac{p}{p_R}), \tag{S19}$$

where $\bar{R} = 8.314\,\frac{\text{kJ}}{\text{kmol K}}$ is the gas constant.

The molar specific entropy at $p_R = 1\,\text{bar}$ is

$$\bar{s}^0(T) = \int_{T_R}^{T} \frac{\bar{c}_p(T')}{T'} dT' + \bar{s}_f^0, \tag{S20}$$

where, $\bar{s}_f^0$ is the chemical species' standard molar entropy at $T_R = 298.15\,\text{K}$, $p_R = 1\,\text{bar}$. Performing the integration gives

$$\bar{s}^0(T) = A \ln\left(\frac{T}{T_R}\right) + B(T - T_R) + C\frac{T^2 - {T_R}^2}{2} + D\frac{T^3 - {T_R}^3}{3} - \frac{E}{2}\left(\frac{1}{T^2} - \frac{1}{{T_R}^2}\right) + \bar{s}_f^0. \tag{S21}$$

The Shomate equations for solid CaO and K_2CO_3 are identical to those given by Eqs. (S15), (S17) and (S21) due to the solids' pressure independence.

For $CaCO_3$, the Shomate equation for molar specific heat is found in Ref. 4 as

$$\bar{c}_p(T) = A + BT + CT^2 + \frac{D}{\sqrt{T}} + \frac{E}{T^2}, \tag{S22}$$

so that molar specific enthalpy and entropy result from integration as

$$\bar{h}(T) = A(T - T_R) + B\frac{T^2 - {T_R}^2}{2} + C\frac{T^3 - {T_R}^3}{3} + 2D\left(\sqrt{T} - \sqrt{T_R}\right) - E\left(\frac{1}{T} - \frac{1}{T_R}\right) + \bar{h}_f^0, \tag{S23}$$

$$\bar{s}(T) = \bar{s}^0(T) \tag{S24}$$

with

$$\bar{s}^0(T) = A \ln\left(\frac{T}{T_R}\right) + B(T - T_R) + C\frac{T^2 - {T_R}^2}{2} - 2D\left(\frac{1}{\sqrt{T}} - \frac{1}{\sqrt{T_R}}\right) - \frac{E}{2}\left(\frac{1}{T^2} - \frac{1}{{T_R}^2}\right) + \bar{s}_f^0. \tag{S25}$$

Table S3: Shomate Constants for All Species

Species	A $\left(\frac{\text{kJ}}{\text{kmol K}}\right)$	B $\left(10^{-3}\frac{\text{kJ}}{\text{kmol K}^2}\right)$	C $\left(10^{-6}\frac{\text{kJ}}{\text{kmol K}^3}\right)$	D $\left(10^{-9}\frac{\text{kJ}}{\text{kmol K}^4}\right)$	E $\left(10^{6}\frac{\text{kJ K}}{\text{kmol}}\right)$
CO_2	24.99735	55.18696	-33.69137	7.948387	-0.136638
O_2	31.32234	-20.23531	57.86644	-36.50624	-0.007374
N_2	28.98641	1.853978	-9.647459	16.63537	0.000117
$H_2O_{(v)}$ $(T < 500\,\text{K})$	32.240	1.923	10.55	-3.95	0
$H_2O_{(v)}$ $(T > 500\,\text{K})$	30.092	6.832514	6.793435	-2.53448	0.082139
CH_4	-0.703029	108.4773	-42.52157	5.862788	0.678565
CaO	49.95403	4.887916	-0.352056	0.046187	-0.825097
K_2CO_3	97.08093	94.22326	-2.053291	0.709644	-0.947860
$CaCO_3$*	-184.79	323.22	-129.74	3883.50**	-3.688200

*For use in Eqs. (S22) through (S24)

**Units $\left(\frac{\text{kJ}}{\text{kmol}\sqrt{\text{K}}}\right)$

Table S4: Molar Masses, Enthalpies of Formation, and Standard Entropies for All Species

Species	$M\left(\frac{\text{kg}}{\text{kmol}}\right)$	$\bar{h}_f^0\left(\frac{\text{kJ}}{\text{kmol}}\right)$	$\bar{s}_f^0\ \left(\frac{\text{kJ}}{\text{kmol K}}\right)$
CO_2	44.0095	-393,522	213.79
O_2	31.9988	0	205.15
N_2	28.0134	0	191.61
$H_2O_{(v)}$	18.0153	-241,830	188.84
CH_4	16.0425	-74,850	186.25
CaO	56.088	-635,090	38.19
K_2CO_3	138.20	-1,150,180	155.44
$CaCO_3$	100.0975	-1,207,600	91.7

Supplemental References

[1] Struchtrup, H. (2014). Thermodynamics and Energy Conversion, 1st Edition. (Springer-Verlag, Berlin, Heidelberg). 10.1007/ 978-3-662-43715-5.

[2] Keith, D.W., Holmes, G., Angelo, D.S., and Heidel, K. (2018). A Process for Capturing CO2 from the Atmosphere. Joule *2*, 1573-1594. 10.1016/j.joule.2018.05.006

[3] Linstrom, P.J. , and Mallard, W.G. (1997). NIST Chemistry WebBook, NIST Standard Reference Database 69 (National Institute of Standards and Technology, Gaithersburg, MD) 10.18434/T4D303.

[4] Jacobs, G.K., Kerrick, D.M., and Krupka, K.M. (1981) The high-temperature heat capacity of natural calcite (CaCO3). Physics and Chemistry of Minerals *7* (2) , 55–59. 10.1007/BF00309451.

[5] Cengel, Y., and Boles, M.(1997) Thermodynamics: An Engineering Approach, 9th Edition (McGraw-Hill, New York, NY).